employed to determine this interaction radius considered only the dispersion forces experienced by pyrene admolecules in the first monolayer on $Al_2O_3(11\bar{2}0)$. The refractive indices contributed by pyrene admolecules above the first monolayer were not taken into account. In contrast, the present model for the average refractive index considers equal contributions from all phenanthrene molecules in the adlayer.

The dispersion interaction radius is also dependent on accurate absolute coverage calibrations. The previous work for pyrene on $Al_2O_3(11\bar{2}0)$ employed a calibrated desorption analysis to determine the pyrene coverages[17] and utilized the measured electronic absorption cross section for pyrene in cyclohexane.[31] Because the line width of the $S_0 \rightarrow S_2$ transition is larger on $Al_2O_3(0001)$ than in cyclohexane, the cross section for pyrene on $Al_2O_3(0001)$ was overestimated by a factor of 3.8. Using the revised absorption cross section and the present model, the previous measurements for pyrene on $Al_2O_3(11\bar{2}0)$ yielded a similar dispersive interaction radius of $r = 18$ Å.

Conclusions

The electronic absorption spectrum of phenanthrene was studied as a function of coverage in disordered adlayers at 20 K on $Al_2O_3(0001)$ and butane multilayer surfaces. The absorption maximum of the $S_0 \rightarrow S_2$ electronic transition shifted from $\lambda = 293$ nm at $\theta = 7$ Å to $\lambda = 301$ nm at $\theta \geq 100$ Å on $Al_2O_3(0001)$. On the butane multilayer surfaces, the absorption maximum red-shifted from $\lambda = 290$ nm at $\theta = 7$ Å to $\lambda = 301$ nm at $\theta \geq 100$ Å. The observed frequency red shifts versus coverage were consistent with dispersion interactions in the phenanthrene adlayer.

Given the magnitude of the frequency shifts relative to the gas-phase transition frequency, the Bayliss equation was employed to calculate the refractive indices in the phenanthrene adlayer as a function of coverage. Refractive indices versus coverage were also determined from the Lorentz–Lorenz equation after calculating the average local density within an interaction sphere centered about each phenanthrene admolecule. The sphere radius of $r = 22$ Å obtained by fitting the calculations to the experimental measurements was in agreement with dispersion interactions.

Acknowledgment. This work was supported by the Office of Naval Research under Contract No. N00014-86-K-737. Some of the equipment used in this work was provided by the NSF-MRL program through the Center for Materials Research at Stanford University. D.R.H. is grateful to the E.K. and Lillian F. Bishop Foundation for partial support. K.R.H. thanks the Natural Sciences and Engineering Research Council of Canada for partial support. N.J.T. thanks the National Science Foundation for a graduate fellowship. S.M.G. acknowledges the National Science Foundation for a Presidential Young Investigator Award and the A.P. Sloan Foundation for a Sloan Research Fellowship.

Registry No. Al_2O_3, 1344-28-1; phenanthrene, 85-01-8; butane, 106-97-8.

Electrostatic Potentials on the Molecular Surfaces of Cyclic Ureides

Jane S. Murray, Pat Lane, Tore Brinck, Peter Politzer,*

Department of Chemistry, University of New Orleans, New Orleans, Louisiana 70148

and Per Sjoberg

Nobel Chemicals, Nobel Industries Sweden, S-691 85 Karskoga, Sweden *(Received: April 23, 1990; In Final Form: July 23, 1990)*

Ab initio SCF–MO electrostatic potentials have been computed at the STO-5G//STO-3G level on the molecular surfaces of a group of cyclic ureides, in order to assess their relative reactivities toward nucleophiles, as in hydrolysis. The surfaces were defined by the 0.002 electron/bohr^3 contour of the molecular electronic density. The relative hydrolytic stabilities within a series of NO_2 and NF_2 derivatives are predicted, on the basis of the magnitudes of the potentials above the acyl carbons. The surface electrostatic potentials of the polycarbonyl systems parabanic acid and alloxan are shown to be fully consistent with unusually short intermolecular distances that have been observed in crystallographic studies of these compounds.

Introduction

Hydrolytic stability is a very important consideration in evaluating both existing and proposed energetic materials. For example, tetranitroglycoluril (Sorguyl, I) shows the desired features of high measured density (2.01 g/cm^3) and detonation velocity (9150 m/s)[1] but suffers from being readily decomposed by hydrolysis.[1] A related compound, dinitroglycoluril (DINGU, II), is stable toward neutral or acidic hydrolysis but easily decomposes under alkaline conditions.[1]

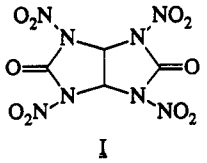

I

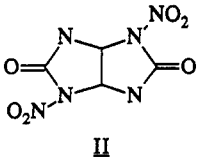

II

For molecules of the general type RC(=O)Ž (III), susceptibility to hydrolysis has been found to correlate with the reactivity of the acyl group, reflecting the resonance structures IIIA–C.[2]

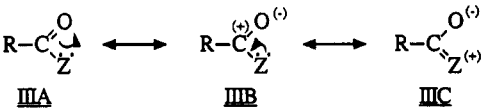

IIIA IIIB IIIC

The greater the contribution of IIIB, the more positive is the acyl carbon, and thus the more reactive it is toward nucleophilic attack, e.g. hydrolysis. We have shown that an effective indicator of the positive nature of the acyl carbon is the electrostatic potential on the surface of the molecule.[3] For example, the surface potentials of acetyl fluoride (IV) and acetamide (V) reveal the acyl carbon

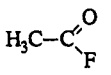

IV

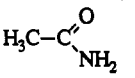

V

in the former to be the more positive, consistent with its exper-

(1) Meyer, R. *Explosives*; VCH Publishers: Weinheim, FRG, 1987.

(2) Allinger, N. L.; Cava, M. P.; De Jongh, D. C.; Johnson, C. R.; Lebel, N. A.; Stevens, C. L. *Organic Chemistry*; Worth Publishers: New York, 1971; Chapter 20.

(3) Sjoberg, P.; Politzer, P. *J. Phys. Chem.* **1990**, *94*, 3959.

0022-3654/91/2095-0844$02.50/0

imentally observed much greater tendency to undergo hydrolysis.[2] Amides, such as V, show a relatively low degree of reactivity toward hydrolysis compared to other carbonyl-containing systems; they require the presence of strong acid or strong base, and often heating as well.[2] This presumably reflects some degree of delocalization of the nitrogen lone pair toward the acyl carbon (structure IIIC).

In this study, we extend our surface electrostatic potential analyses to the more complex cyclic acyl-containing systems VI–XIII. All of these feature the ureido group, >NC(=O)N<,

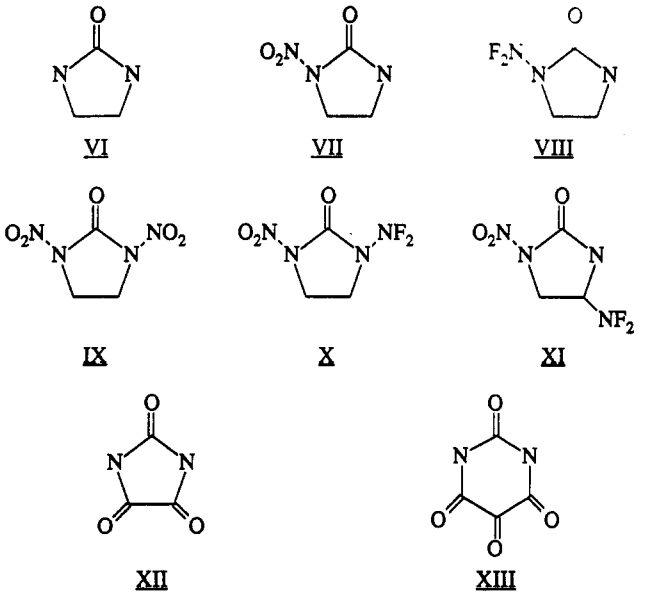

VI VII VIII

IX X XI

XII XIII

which is present also in I and II; indeed, VII and IX can be viewed as building blocks of II and I, respectively. Our objectives are (a) to examine the relative susceptibilities to hydrolysis of the ureido group in various chemical and structural environments and (b) to further explore the use of the surface electrostatic potential as a means for elucidating molecular properties and behavior.

The parent molecule, 2-imidazolidinone (VI), is a structural unit of I and II, as well as of many other existing or proposed energetic systems. The ureides VII–XI are NO_2 and NF_2 derivatives of VI. The NO_2 group is known to be strongly electron-withdrawing, primarily through induction; its inductive substituent constant σ_I is 0.67.[4] σ_I has not been measured for NF_2, but we have recently predicted it to be 0.53.[5] Parabanic acid (XII) and alloxan (XIII) have the interesting feature of being unusually high-density materials; this is particularly true of alloxan. (The measured densities of XII and XIII are 1.72[6] and 1.93 g/cm^3,[7] respectively.)

Methods and Procedure

The electrostatic potential $V(\mathbf{r})$ at any point $\mathbf{r}$ in the space of a molecule is expressed rigorously by eq 1. Z_A is the charge on

$$V(\mathbf{r}) = \sum_A \frac{Z_A}{|\mathbf{R}_A - \mathbf{r}|} - \int \frac{\rho(\mathbf{r}')\, d\mathbf{r}'}{|\mathbf{r}' - \mathbf{r}|} \qquad (1)$$

nucleus A, located at $\mathbf{R}_A$, and $\rho(\mathbf{r})$ is the electronic density function of the molecule, which we obtain by an ab initio self-consistent-field (SCF) molecular orbital approach. The first term on the right side of eq 1 represents the contribution of the nuclei, which is positive; the second term introduces the effect of the electrons, and is negative. An important feature of $V(\mathbf{r})$ is that it is a real physical property, one that can be determined experimentally by diffraction methods as well as computationally.[8]

The electrostatic potential is well-established as an effective tool for interpreting and predicting molecular reactive behavior toward electrophiles[8-10] and for the study of biological recognition interactions.[11,12] An approaching electrophile will go to those regions in which $V(\mathbf{r})$ attains its most negative values (the local minima) since this is where the effects of the molecule's electrons are most dominant (eq 1).

The use of the electrostatic potential to analyze reactivity toward nucleophiles has not been as straightforward as it has been to analyze reactivity toward electrophiles. This can be understood by first recognizing that $V(\mathbf{r})$ for any free neutral atom is positive everywhere, increasing to a maximum at the nucleus.[13-15] This reflects the highly concentrated nature of the nuclear charge as contrasted to the dispersed electronic distribution. When a molecule is formed, the accompanying rearrangement of electrons normally produces one or more regions of negative electrostatic potential. Each negative region has at least one minimum to which an approaching electrophile may be attracted. The positive regions, on the other hand, do not have maxima other than at the positions of the nuclei; these are so large in magnitude that they generally mask any local buildups of positive potential that might indicate sites for nucleophilic attack. We have recently demonstrated that this problem can be avoided by computing $V(\mathbf{r})$ on a three-dimensional surface surrounding the molecule[3] that is sufficiently removed from the nuclei.

In this work, we analyze the electrostatic potential computed on a three-dimensional surface as a guide to nucleophilic attack. Whereas molecular surfaces have often been defined in terms of a set of intersecting "hard spheres" centered on the nuclei,[16-26] we use the molecule's electronic charge distribution to define its surface; the latter is taken to correspond to the 0.002 electron/bohr^3 contour of the molecular electronic density $\rho(\mathbf{r})$. It has been shown, for a group of diatomic molecules and for methane, that this contour gives physically reasonable molecular dimensions, and encompasses at least 95% of the electronic charge.[27,28] Since

(4) Exner, O. *Correlation Analysis of Chemical Data*; PNS: Prague, 1988.
(5) Sjoberg, P.; Murray, J. S.; Brinck, T.; Politzer, P. *Can. J. Chem.* **1990**, *68*, 1440.
(6) Davies, D. R.; Blum, J. J. *Acta Crystallogr.* **1955**, *8*, 129.
(7) Bolton, W. *Acta Crystallogr.* **1964**, *17*, 147.
(8) Politzer, P.; Truhlar, D. G., Eds. *Chemical Applications of Atomic and Molecular Electrostatic Potentials*; Plenum Press: New York, 1981.
(9) Politzer, P.; Daiker, K. C. In *The Force Concept in Chemistry*; Deb, B. M., Ed.; Van Nostrand Reinhold: New York, 1981; p 294.
(10) Scrocco, E.; Tomasi, J. *Adv. Quantum Chem.* **1978**, *11*, 115.
(11) Politzer, P.; Laurence, P. R.; Jayasuriya, K. *Environ. Health Perspect.* **1985**, *61*, 191 (Special Issue on Structure-Activity Correlation in Mechanism Studies and Procedure Toxicology).
(12) Politzer, P.; Murray, J. S. In *Theoretical Biochemistry and Molecular Biophysics: A Comprehensive* Survey; Beveridge, D. L.; Lavery, R., Eds.; Adenine Press: Guilderland, NY; in press.
(13) Politzer, P.; Parr, R. G. *J. Chem. Phys.* **1974**, *61*, 4268.
(14) Weinstein, H.; Politzer, P.; Srebrenik, S. *Theor. Chim. Acta* **1975**, *38*, 159.
(15) Politzer, P. In *Homoatomic Rings, Chains and Macromolecules of Main-Group Elements*; Rheingold, A. L., Ed.; Elsevier: New York, 1977; Chapter 4.
(16) Pullman, B.; Perahia, D.; Cauchy, D. *Nucleic Acids Res.* **1979**, *6*, 3821.
(17) Weiner, P. K.; Langridge, R.; Blaney, J. M.; Schaefer, R.; Kollman, P. A. *Proc. Natl. Acad. Sci. U.S.A.* **1982**, *79*, 709.
(18) Connolly, M. L. *Science* **1983**, *221*, 709.
(19) Bash, P. A.; Pattabiraman, N.; Huang, C.; Ferrin, T. E.; Langridge, R. *Science* **1983**, *222*, 1325.
(20) Francl, M. M.; Hout, R. F., Jr.; Hehre, W. J. *J. Am. Chem. Soc.* **1984**, *106*, 563.
(21) Quarendon, P.; Naylor, C. B.; Richards, W. G. J. *J. Mol. Graphics* **1984**, *2*, 4.
(22) Connolly, M. L. *J. Am. Chem. Soc.* **1985**, *107*, 1118.
(23) Ritchie, J. P. *J. Am. Chem. Soc.* **1985**, *107*, 1829.
(24) Burridge, J. M.; Quarendon, P.; Reynolds, C. A.; Goodford, P. J. *J. Mol. Graphics* **1987**, *5*, 165.
(25) Arteca, G. A.; Jammal, V. B.; Mezey, P. G.; Yadav, J. S.; Hermsmeier, M. A.; Gund, T. M. *J. Mol. Graphics* **1988**, *6*, 45.
(26) Kahn, S. D.; Parr, C. F.; Hehre, W. J. *Int. J. Quantum Chem., Quantum Chem. Symp.* **1988**, *22*, 575.
(27) Bader, R. F. W.; Henneker, W. H.; Cade, P. E. *J. Chem. Phys.* **1967**, *46*, 3341.

TABLE I: Calculated Properties of Acyl Carbons

molecule	$V_{S,C}$, kcal/mol	atomic charges
 VI	+14.6	+0.304
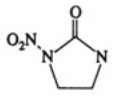 VII	+31.9	+0.401
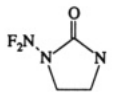 VIII	+24.4	+0.403
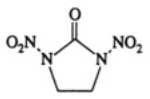 IX	+45.3	+0.404
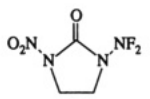 X	+35.0	+0.408
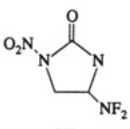 XI	+34.4	+0.411
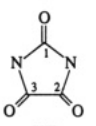 XII	+28.5 (C1) +30.3 (C2) +30.3 (C3)	+0.435 (C1) +0.307 (C2) +0.307 (C3)
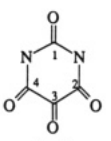 XIII	+30.9 (C1) +35.0 (C2) +37.1 (C3) +35.0 (C4)	+0.434 (C1) +0.303 (C2) +0.169 (C3) +0.303 (C4)

this surface is defined in terms of the molecular property $\rho(\mathbf{r})$, it reflects features such as bond formation, lone pairs, etc. that are unique to a molecule.

For each of the molecules of interest (VI–XIII), geometry optimizations were carried out at the STO-3G level by using the ab initio SCF molecular orbital program GAUSSIAN 82.[29] These geometries were then used to compute the STO-5G electronic densities used to define our molecular surfaces and to compute $V(\mathbf{r})$ on these surfaces. (We have found the STO-5G basis set to be reliable for properties related to the electronic density, such as $V(\mathbf{r})$.) We also include in our analysis the STO-5G atomic charges of the acyl carbons of VI–XIII, calculated by using Mulliken's population analysis procedure.[30]

Results

In this study, we present and analyze surface electrostatic potential data for VI–XIII. Our focus is primarily on the relative magnitudes of the electrostatic potentials on the surfaces of these systems, in the vicinities of the acyl carbons. These $V(\mathbf{r})$ values in conjunction with the overall surface $V(\mathbf{r})$ patterns are used to predict relative susceptibilities toward nucleophilic attack, as in hydrolysis.

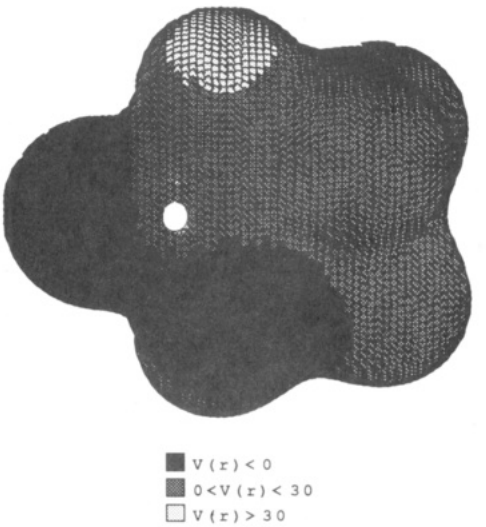

Figure 1. Calculated electrostatic potential on the molecular surface of 2-imidazolidinone (VI). The ranges of $V(\mathbf{r})$ are given below the diagram, in kcal/mol. The white circle is directly above the acyl carbon; the electrostatic potential at this point is $V_{S,C}$.

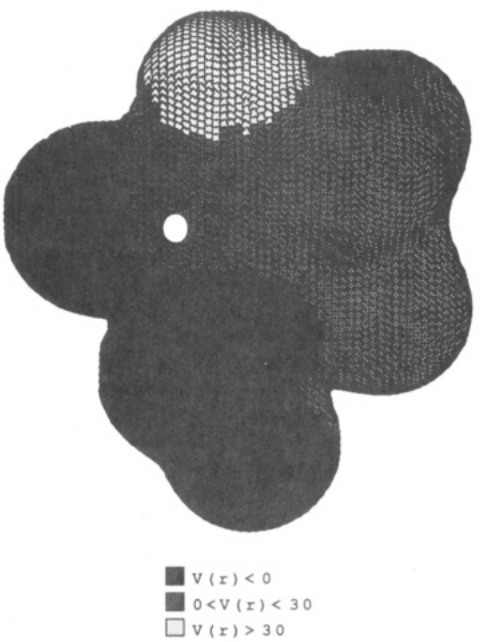

Figure 2. Calculated electrostatic potential on the molecular surface of 1-(difluoroamino)-2-imidazolidinone (VIII). The ranges of $V(\mathbf{r})$ are given below the diagram, in kcal/mol. The white circle is directly above the acyl carbon; the electrostatic potential at this point is $V_{S,C}$.

Table I lists the $V(\mathbf{r})$ values on the surfaces of VI–XIII directly above the acyl carbons, designated as $V_{S,C}$, and also the calculated acyl carbon atomic charges. The surface potential of 2-imidazolidinone (VI), which has the lowest calculated $V_{S,C}$ in Table I, is shown in Figure 1. There is an overlap of the regions of negative potential associated with the oxygen and nitrogen lone pairs. (One nitrogen lone-pair region projects toward the viewer in Figure 1; the other faces away.) The acyl carbon of VI is thus significantly shielded by negative potential.

The introduction of the electron-withdrawing NO_2 and NF_2 groups, to give VII and VIII, diminishes the lone-pair regions of the substituted ring nitrogens (compare Figures 1 and 2) and makes $V_{S,C}$ more positive (Table I). These effects are more pronounced for the more strongly electron-withdrawing NO_2.

Of the three disubstituted imidazolidinone systems IX–XI, the dinitro derivative (IX) has the most positive $V_{S,C}$, +45.3 kcal/mol. The surface $V(\mathbf{r})$ of IX, presented in Figure 3, has smaller nitrogen

(28) Bader, R. F. W.; Preston, H. J. T. *Theor. Chem. Acta* **1970**, *17*, 384.
(29) Binkley, J. S.; Frisch, M. J.; DeFrees, D. J.; Krishnan, R.; Whiteside, R. A.; Schlegel, H. B.; Fluder, E. M.; Pople, J. A. *GAUSSIAN 82*, Carnegie-Mellon Quantum Chemistry Publishing Unit: Pittsburgh, PA 15213.
(30) Mulliken, R. S. *J. Chem. Phys.* **1955**, *23*, 1833.

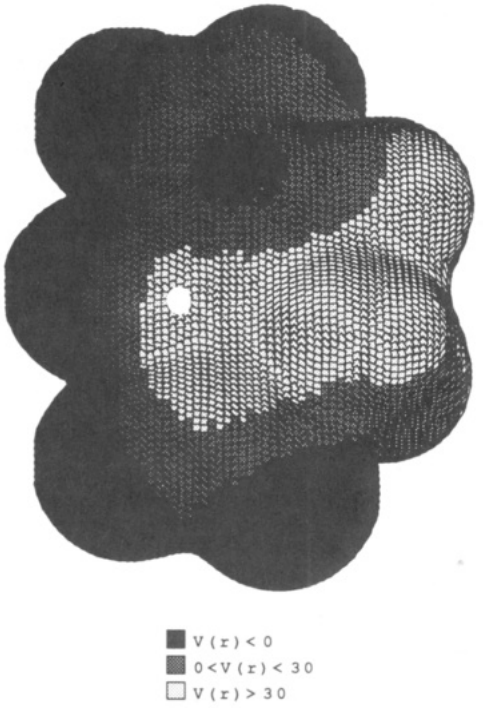

Figure 3. Calculated electrostatic potential on the molecular surface of 1,3-dinitro-2-imidazolidinone (IX). The ranges of $V(\mathbf{r})$ are given below the diagram, in kcal/mol. The white circle is directly above the acyl carbon; the electrostatic potential at this point if $V_{S,C}$.

lone-pair regions and a larger, more positive $V(\mathbf{r})$ surface area than the unsubstituted and monosubstituted systems VI–VIII. (See Figures 1 and 2 for comparison.) The surface potentials of X and XI have patterns qualitatively similar to that of IX; however their positive regions are considerably weaker, their $V_{S,C}$ values being in the range 34–35 kcal/mol. It is interesting that the NO_2, NF_2 combination produces a $V_{S,C}$ that is only slightly more positive than that due to a single NO_2 and that $V_{S,C}$ is essentially independent of whether the NF_2 is on a ring nitrogen or carbon.

Table I shows that the degrees of positive character of the acyl carbons in parabanic acid (XII) and alloxan (XIII) correlate inversely with their proximities to the ring nitrogens, presumably reflecting delocalization of the nitrogen lone pairs. Thus the least positive carbon in each molecule is the one between the two nitrogens.

The surface $V(\mathbf{r})$ patterns of XII and XIII are quite similar; the latter is shown in Figure 4. It is interesting to compare the surface potential of XIII with that of VI (Figure 1). These are both unsubstituted molecules, but the surface of XIII is much more positive. The oxygen negative regions are smaller in the latter, and the nitrogen lone pairs do not even show up as negative on the molecular surface, attesting to the extent of their delocalization. Indeed the potential over the central part of XIII approaches that of IX (which has two strongly electron-withdrawing NO_2 groups), and even exceeds it on some portions of the surface, where the ring nitrogens of the latter do retain small negative regions (Figure 3). The high degree of reactivity of C3 in XIII toward nucleophiles is shown by the fact that alloxan readily combines with atmospheric moisture to give XIV.[7]

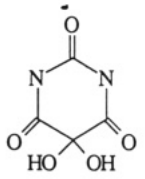

XIV

Discussion

Our calculated surface $V(\mathbf{r})$ results provide a basis for predicting the relative hydrolytic tendencies of the 2-imidazolidinones VI–XI.

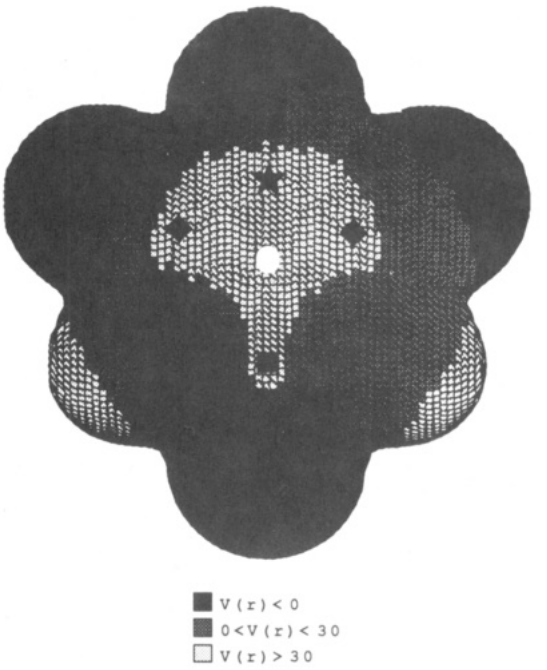

Figure 4. Calculated electrostatic potential on the molecular surface of alloxan (XIII). The ranges of $V(\mathbf{r})$ are given below the diagram, in kcal/mol. The location of the maximum potential, +47.6 kcal/mol, is indicated by the white circle. The $V_{S,C}$ values are (★) +37.1; (◆) +35.0; and (■) +30.9 kcal/mol.

Susceptibility toward hydrolysis is expected to increase roughly as $V_{S,C}$ becomes more positive. Accordingly, the dinitro derivative, IX, is expected to show the greatest propensity to hydrolyze, and the instability of I can readily be understood. It is to be anticipated that the number of C=O groups in the molecule is also an important factor in determining its reactivity, since each of them is a potential site for nucleophilic interaction. Thus XII might well have a greater tendency to hydrolyze than VII.

Table I shows that while the NF_2 substituent alone produces a considerable increase in $V_{S,C}$ (as in VIII), the effect of NF_2 and NO_2 together is only slightly greater than that of NO_2 alone (X and XI). This is believed to reflect the fact that the polarizable electronic charge is now subject to the inductive powers of both of these substituents, and accordingly the response to each of them is less than if that substituent were alone. Our finding $V_{S,C}$ to be essentially the same for both X and XI can be attributed to the primarily inductive (rather than conjugative) electron-withdrawing effect of NF_2.

Parabanic acid, XII, and alloxan, XIII, are two members of a small group of cyclic polycarbonyl molecules that are characterized, in the crystalline form, by some unusually short intermolecular O=C···O=C separations.[7,31] These C···O distances reach values as low as 2.77 Å in XII[6] and 2.79 Å in XIII,[7] whereas the sum of the carbon and oxygen van der Waals radii is approximately 3.1 Å.[32] The resulting closely packed three-dimensional structure is presumably the reason for the unusually high densities of these compounds.[7,33] These close distances of approach, which involve C2 (or C3) in XII and C3 in XIII, have been attributed to dipole interactions by Bolton[7,31] and to deshielding of the carbon nucleus (in XIII) by Swaminathan et al.[33]

Our results are quite consistent with the crystallographic observations and help to clarify the physical situation. We find that the most positive potential on the parabanic acid surface is 37.3 kcal/mol, at a projected position in the molecular plane about 1.00 Å from both C2 and C3, on the perpendicular bisector of the C2–C3 axis. On the alloxan surface, the maximum is stronger, 47.6 kcal/mol, and its projected position is approximately 1.34

(31) Bolton, W. *Nature* **1964**, *201*, 987.
(32) Bondi, A. *J. Phys. Chem.* **1964**, *68*, 441.
(33) Swaminathan, S.; Craven, B. M.; McMullan, R. K. *Acta Crystallogr.* **1985**, *B41*, 113.

Å from C3 on the C1–C3 axis (Figure 4). The crystallographic analyses of parabanic acid and alloxan show that the C···O=C angles corresponding to the closest intermolecular distances are 157.4 and 154.7°, respectively;[7,31] the corresponding projected positions of the oxygens on the molecular planes of XII and XIII are 1.06 Å from C2 and C3 for the former and 1.19 Å from C3 for the latter. Thus these oxygens, which are negative (Figure 4), are near the most positive regions of the surface potentials, and the resulting electrostatic interactions can accordingly account for the short internuclear distances.

Finally, it should be noted that the calculated atomic charges listed in Table I bear little or no relationship to the $V_{S,C}$ values. For example, the dinitro derivative IX, which has the largest $V_{S,C}$ in the table, has only an average acyl carbon charge. Even more striking are the ordering and range of magnitudes of the acyl carbon charges in parabanic acid and alloxan, which do not show at all the same trends as do the surface potentials. In alloxan, the carbon with the largest $V_{S,C}$ is C3, which has the lowest charge in all of Table I. These observations are consistent with the absence of a reliable correlation between calculated atomic charges and chemical reactivity.[9,34,35]

Summary

We have investigated the susceptibilities toward nucleophilic attack, e.g. hydrolysis, of a group of cyclic ureides. We examined the surface electrostatic potentials of these molecules, focusing upon the regions above the acyl carbons, to determine the effects of various chemical and structural modifications, including the presence of NO_2 and/or NF_2 substituents. The relative hydrolytic stabilities of these systems have been predicted. For the polycarbonyl molecules parabanic acid and alloxan, the magnitudes and locations of the maxima in their surface potentials are fully consistent with observed unusually short intermolecular distances in their crystalline forms.

Acknowledgment. We thank Dr. Jorge M. Seminario and Mrs. Monica Concha for computational assistance. We greatly appreciate the support of this work by the Office of Naval Research through Contract No. N00014-85-K-0217.

(34) Julg, A. In *Topics in Current Chemistry*; Springer-Verlag: Berlin, 1975; Vol. 58.
(35) Polak, R. *Theor. Chim. Acta* **1978**, *50*, 21.

Mobility of Adsorbed Species in Zeolites: Methane, Ethane, and Propane Diffusivities

A. K. Nowak,[†] C. J. J. den Ouden,*[,‡] S. D. Pickett,[†] B. Smit,[‡] A. K. Cheetham,[§] M. F. M. Post,[‡] and J. M. Thomas[†]

Davy Faraday Research Laboratory, The Royal Institution, 21 Albemarle Street, London W1X 4BS, United Kingdom, Koninklijke/Shell-Laboratorium, Amsterdam (Shell Research B.V.), Badhuisweg 3, 1031 CM Amsterdam, The Netherlands, and Chemical Crystallography Laboratory, University of Oxford, 9 Parks Road, Oxford OX1 3PD, United Kingdom *(Received: February 8, 1990; In Final Form: August 17, 1990)*

Molecular dynamics simulations were performed in order to study the influence of the zeolite structure on molecular migration in the zeolitic void space. The migration of methane in various zeolitic environments was examined by using the all-silica polymorphs of zeolite EU-1, mordenite, and silicalite. Furthermore, diffusion simulations of ethane and propane in silicalite were carried out and computed diffusion characteristics were compared with experimental data.

Introduction

Computer simulations of adsorption and diffusion in zeolites have gained much interest over the last few years. This increasing interest is due to the notion that simulations may offer new insights into adsorption and diffusion phenomena that are of direct importance in studies on the catalytic activity and selectivity of zeolites.

Limitations arising from insufficient computer power hindered the application of computer simulations in the past. However, thanks to the advances made in the development of computer hardware and methodologies of computational chemistry, computer simulations now offer a valuable contribution to zeolite catalysis research.

Several adsorption and diffusion simulations in zeolites have been carried out recently. The first simulations, based on simple potential energy minimizations, identified preferred adsorption sites or potential energy maps of the zeolite inner void space.[1-4] Later, Monte Carlo (MC) simulations were employed to study the average siting of methane in zeolite Y[5] and in the zeolites ZSM-5 and mordenite;[6] Leherte et al.[7] studied concentration effects on water adsorption in ferrierite.

More recently, molecular dynamics (MD) simulations have been applied to determine time-dependent properties such as diffusion coefficients and intracrystalline site residence times for methane in the zeolites Y,[8] mordenite,[9] A,[10] and ZSM-5,[9,11] for benzene

* Author to whom correspondence should be addressed.
† The Royal Institution.
‡ Koninklijke/Shell-Laboratorium.
§ University of Oxford.

(1) Bezus, A. G.; Kiselev, A. V.; Lopatkin, A. A.; Du, P. Q. *J. Chem. Soc., Faraday Trans. 2* **1978**, *74*, 367. Kiselev, A. V.; Du, P. Q. *J. Chem. Soc., Faraday Trans. 2* **1981** *77*, 1. Kiselev, A. V.; Du, P. Q. *J. Chem. Soc., Faraday Trans. 2* **1981** *77*, 17. Kiselev, A. V.; Lopatkin, A. A.; Shulga, A. A. *Zeolites* **1985**, *5*, 261.
(2) Wright, P. A.; Thomas, J. M.; Cheetham, A. K.; Nowak, A. K. *Nature* **1985**, *318*, 611.
(3) Muller, U.; Unger, K. K.; Dongfeng, P.; Mersman, A.; Grillet, Y.; Rouquerol, F.; Rouquerol, J. In Zeolites as Catalysts, Sorbents and Detergent Builders. *Studies in Surface Science and Catalysis*; Weitkamp, J., Karge, H. G., Eds.; Elsevier: Amsterdam, (1989; Vol. 46, p 625.
(4) Nowak, A. K.; Cheetham, A. K.; Pickett, S. D.; Ramdas, S. *Molecular Simulation* **1987**, *1*, 67.
(5) Yashonath, S.; Thomas, J. M.; Nowak, A. K.; Cheetham, A. K. *Nature* **1988**, *331*, 601.
(6) Smit, B.; Den Ouden, C. J. J. *J. Phys. Chem.* **1988**, *92*, 7169.
(7) Leherte, L.; Vercauteren, D. P.; Derouane, E. G.; Andre, J. M. In Innovation in Zeolite Materials Science. *Studies in Surface Science and Catalysis*; Grobet, P. J., Mortier, W. J., Vansant, E. F., Schulz-Ekloff, G., Eds.; Elsevier: Amsterdam, 1988, Vol. 37, p 293.
(8) Yashonath, S.; Demontis, P.; Klein, M. L. *Chem. Phys. Lett.* **1988**, *153* (6), 551.
(9) Den Ouden, C. J. J.; Smit, B.; Wielers, A. F. H.; Jackson, R. A.; Nowak, A. K. *Molecular Simulation* **1989**, *4*, 121.
(10) Cohen De Lara, F.; Kahn, R.; Goulay, A. M. *J. Chem. Phys.* **1989**, *90* (12), 7482.

0022-3654/91/2095-0848$02.50/0